Chem. Res. Chinese Universities, 2020, 36(4), 511—517 doi: 10.1007/s40242-020-0188-x

Review

# Growth of Single-crystalline Transition Metal Dichalcogenides Monolayers with Large-size

ZHOU Shengxue[1,2] and JIAO Liying[1*]

*1. Key Laboratory of Organic Optoelectronics and Molecular Engineering of Ministry of Education, Department of Chemistry, Tsinghua University, Beijing 100084, P. R. China;*

*2. Department of Chemistry and Chemical Engineering, Ningxia Normal University, Guyuan 756000, P. R. China*

**Abstract** Two-dimensional(2D) transition metal dichalcogenides(TMDCs) semiconductors, such as monolayers of molybdenum disulfide($MoS_2$) and tungsten disulfide($WS_2$) can potentially serve as ultrathin channel materials for building short channel field-effect transistors(FETs) to further extend Moore's Law. It is essential to develop controllable approaches for the synthesis of large single crystals of these 2D semiconductors to promote their practical applications in future electronics. In this short review, we summarized the recent advances on the chemical vapor deposition(CVD) of single crystalline semiconducting 2D TMDCs with a large size. We first discussed the driving force and urgent demands on developing controllable approaches for the growth of large 2D TMDCs single crystals and then summarized the current strategies and representative studies on the CVD growth of large 2D single crystals. Finally, we discussed the challenges and future directions in this topic.

**Keywords** Two dimensional; Single crystal; Chemical vapor deposition; Field effect transistor

## 1 Introduction

In recent years, the further scaling of silicon-based transistors confronts great challenges[1—3]. Although silicon based semiconductors still have a strong vitality[4,5], it is extremely urgent to explore new semiconducting materials. In the past two decades, low-dimensional semiconducting materials, such as single-walled carbon nanotubes(SWNTs) and two-dimensional(2D) semiconductors, such as several transition metal dichalcogenides(TMDCs) have attracted extensive attentions, showing great potentials in the application of electronic devices in the future.

2D semiconductors, such as $MoS_2$ are highly ordered single crystals without danging bonds on the surface, showing a band gap between 0.2 eV and 2.1 eV[6,7] and more importantly, they are ultra thin semiconductors with a thickness of down to *ca.* 0.65 nm, and therefore, are expected to overcome the short-channel effect[8—14], which limited the further scaling of silicon-based transistors. In addition, 2D TMDCs semiconductors have various chemical compositions and structures, thus showing abundant and unique properties[15—19]. The band structures and electrical characteristics of such materials can be modulated by engineering the number of layers[20], phases[21], defects[22], and so on, and be allowed for the construction of electronic devices with these tunable 2D building blocks[23—26]. For example, $MoS_2$ in 1T′ phase[21] shows metallic properties, which is totally different from its semiconducting counterparts of 2H phase $MoS_2$, and 2D $PtSe_2$ exhibits obviously layer-dependent electrical properties and catalytic activity[27]. However, for device applications, it is essential to achieve the controlled synthesis of such ultra thin 2D single crystals.

## 2 Potential Applications of TMDCs in Electronic Devices and Integrated Circuits

### 2.1 Application of 2D TMDCs in Field-effect Transistors

Semiconducting 2D TMDCs, such as $MoS_2$, $MoSe_2$, $WS_2$ and $WSe_2$, owning wide band gaps, ultra-thin 2D planar structures, excellent electrical properties, and low dielectric constants, are ideal channel materials for constructing field-effect transistors(FETs)[28—31]. Compared with silicon-based materials, the thickness of 2D TMDCs can be reduced to sub-nanometer[26], showing the potential to further extend Moore' Law. In 2011, Kis *et al.*[32] successfully fabricated top-gated FETs by using hafnium dioxide($HfO_2$) as the dielectries layer and mechanically exfoliated single-layered $MoS_2$ as the channel material. The obtained FETs exhibited an on/off current ratio of *ca.* $10^8$ and a subthreshold slope of *ca.* 70 mV/decade[Fig.1(A) and (B)]. Subsequently, Wei *et al.*[33] fabricated FETs with exfoliated $WS_2$ as channel material and the mobility at room temperature could reach up to 200 $cm^2 \cdot V^{-1} \cdot s^{-1}$

*Corresponding author. Email: lyjiao@tsinghua.edu.cn

Received June 15, 2020; accepted July 8, 2020.

Supported by the National Natural Science Foundation of China(Nos.21875127, 21925504) and the Tsinghua University Initiative Scientific Research Program, China.

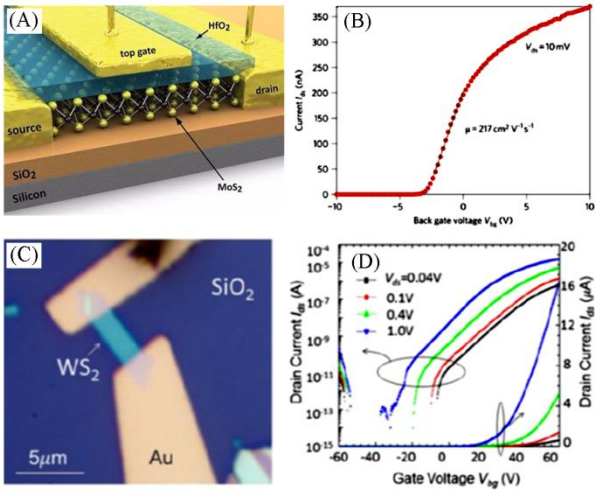


**Fig.1 Schematics of a top-gated FET with single-layered $MoS_2$ as the channel material(A)[32], typical transfer characteristic curve of the top-gated $MoS_2$ FET(B)[32], optical image of an FET fabricated with exfoliated multilayered $WS_2$(C)[33] and transfer characteristics curves of the FET shown in (C)(D)[33]**

(A, B) Copright 2011, Nature Nanotechnology; (C, D) Copright 2014, ACS Nano.

[Fig.1(C) and (D)]. Chai *et al.*[34] fabricated FETs with the channel material of monolayer $PtSe_2$ exfoliated from bulk crystals grown by the chemical vapor transport(CVT) method, showing an intrinsic high-mobility of *ca.* 210 $cm^2 \cdot V^{-1} \cdot s^{-1}$. And they realized the carrier type control in $WSe_2$-FETs by thickness modulation, obtained p-type, ambipolar and n-type with the thickness below 4 nm, *ca.* 6 nm and over 15 nm, respectively[35]. These works and more subsequent researches[36—41] opened up the intensive studies on the construction and optimization of 2D TMDCs based FETs in recent years and demonstrated the promise of 2D semiconductors in high performance field effect devices.

## 2.2 2D TMDCs for the Construction of Short-channel Devices

As the main driving force for the studies on 2D semiconductors is to further decrease the channel length of FETs, Javey *et al.*[42] demonstrated the fabrication of FETs with a gate length of only 1 nm by using a double-layered $MoS_2$ as the channel, a single-wall carbon nanotube with a diameter of 1 nm as the gate, and a 5-nm thick zirconia($ZrO_2$) as the dielectrics, as shown in Fig.2(A). The on/off current ratio of the as-prepared transistors reached *ca.* $10^6$, and the subthreshold slope reached 65 mV/decade[Fig.2(B)], which was close to the theoretical limit. These results confirmed that $MoS_2$ had a good immunity to short channel effect, which was consistent with the theoretical calculations[43,44]. Although the device prepared by this method is still at the prototype stage, it fully demonstrates the feasibility of using $MoS_2$ and other 2D TMDCs to construct electronic devices in nanoscale.

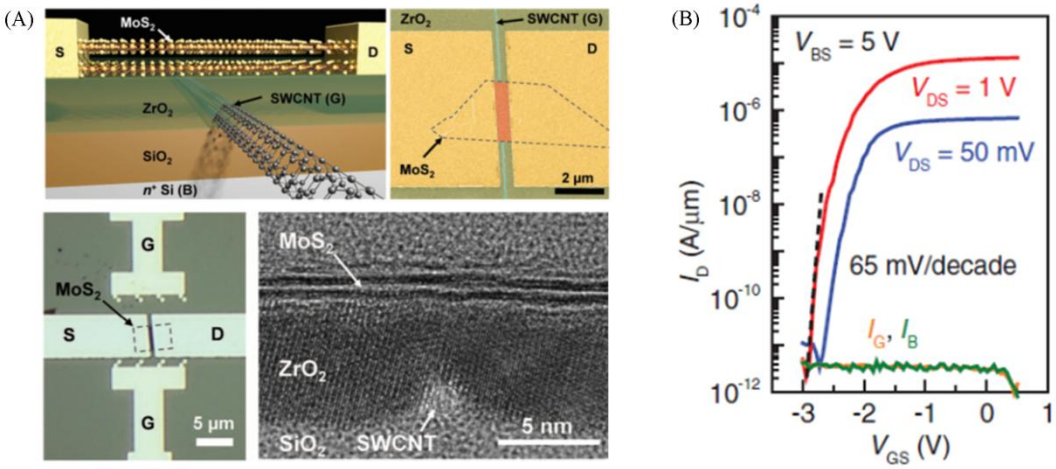


**Fig.2 FETs with $MoS_2$ as channel and single-wall carbon nanotubes as gate(A) and its $I_D$-$V_{GS}$ transfer characteristic curves(B)[42]**

Copyright 2016, Science.

## 2.3 Challenges of 2D TMDCs for Device Integration

Currently, due to the size limitation of the obtained single crystals of 2D TMDCs, the fabrication of large arrays of electronic devices with 2D semiconductors are mainly based on polycrystalline films. Park *et al.*[45] synthesized polycrystalline $MoS_2$ film *via* metal-organic chemical vapor deposition (MOCVD) on a 4-inch silicon wafer, and prepared a large FETs array based on this polycrystalline film[Fig.3(A) and (B)], in which *ca.* 99% of the devices worked normally. Duan *et al.*[46] fabricated large arrays of FETs on polycrystalline $MoS_2$ film prepared by solution phase exfoliation, and further constructed logic circuits[Fig.3(C)—(E)]. Mueller *et al.*[47] prepared photodiode arrays over a large area with few-layered $WSe_2$ [Fig.3(F)—(H)] and realized rapid image recognition. Although the channel materials are not single crystals, these results have shown the great potential of 2D TMDCs in device integration.

Both experimental studies and theoretical calculations suggested that the abundant grain boundaries and defects in polycrystalline 2D TMDCs dramatically limited their electrical transport capabilities[48]. Therefore, it is critical and urgent to develop controllable synthesis approaches to enlarge the size

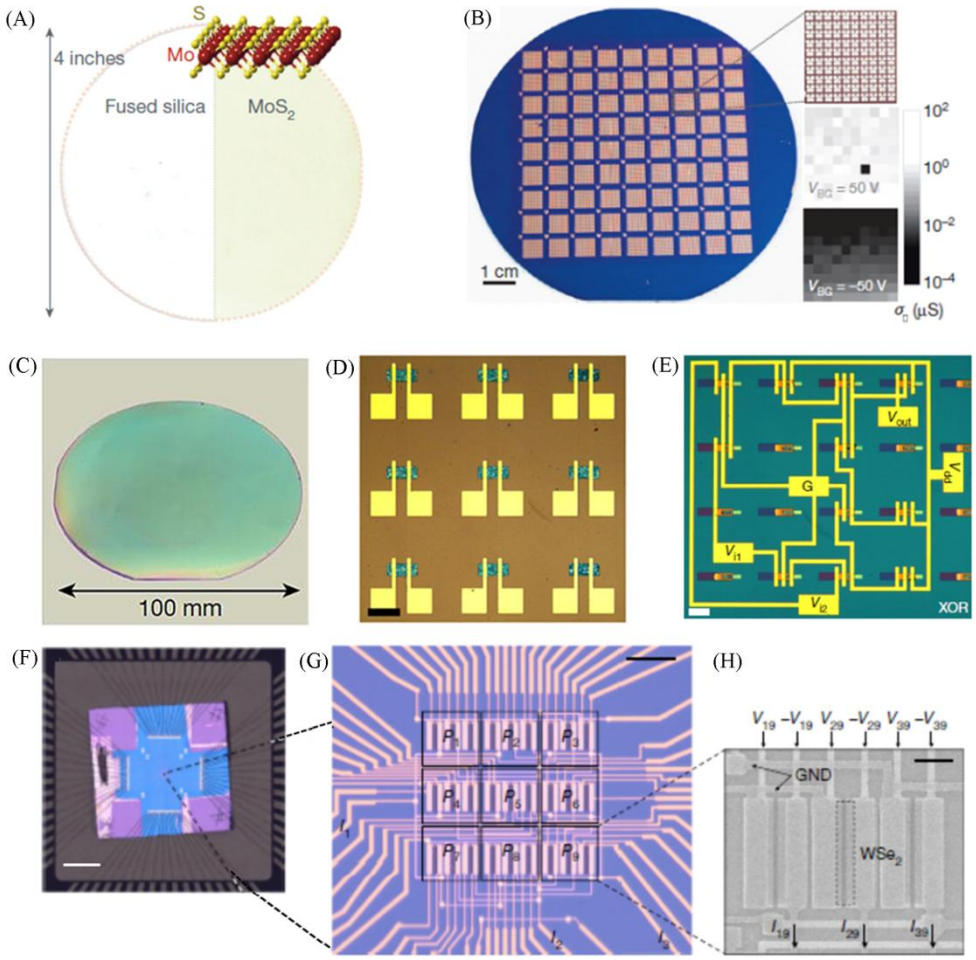


**Fig.3 Devices arrays fabricated with 2D TMDCs polycrystalline films**

(A) Optical image of the as-grown $MoS_2$ polycrystalline film; (B) the FETs arrays fabricated on the film shown in (A)[45]; (C) $MoS_2$ polycrystalline film prepared by liquid phase method; (D) the obtained transistor array; (E) the logic circuit, scale bars in (D) and (E): 100 μm[46]; (F)—(H) images of the device arrays using $WSe_2$ as channel material at different magnifications[47], scale bars in (F)—(H): 2 mm, 15 μm and 3 μm, respectively.

(A, B) Copyright 2015, Nature; (C—E) Copyright 2018, Nature; (F—H) Copyright 2020, Nature.

of the single crystals of 2D semiconductors to promote their practical applications in electronic devices.

## 3 Recent Advances on the CVD Growth of Large Single-crystal of 2D TMDCs

Among various preparation methods, some solution-phase preparation approaches are capable of producing TMDCs monolayers with size of over 100 μm[49,50] and hold the promise for large scale production. While 2D TMDCs synthesized by vapor phase deposition approaches, such as chemical vapor deposition(CVD), physical vapor deposition(PVD)[51], chemical vapor transport(CVT)[15,52] and molecular beam epitaxy(MBE)[53] are suitable for applications in electronic devices as the growth is conducted on the gas-solid interfaces and can avoid the surface contamination of the obtained 2D materials to the largest extent. CVD method is widely used for the controlled synthesis of low dimensional materials and is capable of growing high quality single crystals of 2D TMDCs and moreover, this approach holds the promise of commercialization and therefore, we will focus on the growth of single crystals of TMDCs monolayers with CVD approach in this review.

### 3.1 Conventional CVD Growth of 2D TMDCs

In 2009, Ruoff *et al.*[54] synthesized monolayers of graphene on Cu foils by CVD method. Afterwards, CVD method was applied to the synthesis of 2D TMDCs. The method of *in-situ* synthesis of $MoS_2$ was first performed by thermal decomposition of $(NH_4)_2MoS_4$ thin film. Li *et al.*[55] soaked the substrate in $(NH_4)_2MoS_4$ solution, and heated it at 500 °C in $Ar/H_2$ atmosphere for 1 h. Then the atmosphere was adjusted to Ar or Ar/S for 30 min at 1000 °C, and obtained polycrystalline film on sapphire and $SiO_2$/Si substrates, respectively[Fig.4(A)]. Another synthesis strategy of 2D $MoS_2$ is based on the surface growth of atomic layers of $MoS_2$ by using $MoO_3$ and S as growth precursors as shown in Fig.4(B). $MoO_3$ and S were vaporized in the CVD furnace and reacted in the gas phase at a high temperature to form $MoS_2$ or the intermediate products of $MoS_{2-x}O_x$ and then the products deposited on the growth substrates as nucleuses and grew up into triangular flakes with a side length of a few micrometers to *ca*. 100 μm[Fig.4(C)][56,57].

The obtained monolayered $MoS_2$ flakes were fabricated into FETs and showed electron mobility of 1—8 $cm^2 \cdot V^{-1} \cdot s^{-1}$, comparable to the mechanically exfoliated samples. Compared with the *in-situ* conversion method, the surface growth mode is more suitable for the synthesis of single crystals of 2D TMDCs.

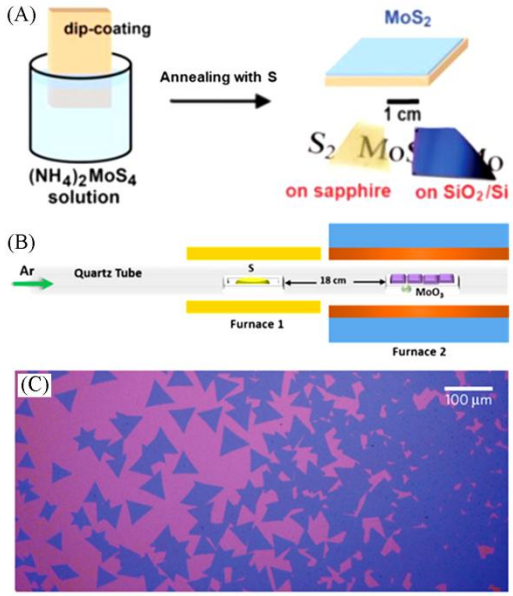


**Fig.4 CVD growth of 2D TMDCs**

(A) Schematics for the *in-situ* synthesis of $MoS_2$ by thermal decomposition of $(NH_4)_2MoS_4$ and optical images of the product[55]; (B) schematics for the typical set-up of the CVD growth of $MoS_2$ by using $MoO_3$ and S as the growth precursors[56]; (C) typical optical image of $MoS_2$ flakes grown on $SiO_2$/Si substrate[57].

(A) Copyright 2012, Nano Letters; (B) Copyright 2014, Chemistry of Materials; (C) Copyright 2013, Nature.

## 3.2 Large-size Growth of 2D TMDCs Single Crystals

The surface growth of 2D TMDCs by CVD allows for the synthesis of highly crystalline $MoS_2$ and other 2D TMDCs on various substrates. For practical applications of 2D TMDCs in integrated circuits, the sizes of the samples should reach up to wafer scale. However, currently, the sizes of the obtained 2D single crystals are usually below 100 μm. As many growth parameters, such as the growth precursors, substrates, growth temperatures, pressures, flow rates of the carrier gas and so on can affect the growth results and the detailed growth mechanism is still unclear at the current stage, it is still challenging to further increase the size of the 2D single crystals. And a lot of related studies are still in progress.

Here we defined 'large-size' as above 100 μm and summarized the recent studies on growing 2D TMDCs single crystals larger than 100 μm by CVD method roughly from the following aspects: nucleation control, increase the growth rates and surface engineering.

### *3.2.1 Nucleation Control*

For the growth of the large single crystals of 2D TMDCs, it is straight forward to decrease the nucleation density and ideally, form only one nucleus on the substrates to allow for the growth of the largest single crystal on the substrate. During the growth of 2D materials, nucleuses are usually formed at a high energy site on the substrate surface[58]. In the absence of effective control, the distribution and orientation of crystal nucleuses on the substrate are often random, which will lead to a large number of grain boundaries when different crystal domains grow up and merge together. Therefore, the suppression of nucleation is an effective strategy to realize high quality 2D single crystal growth from mono-nucleus. Loh *et al.*[59] employed a molten glass as substrate, which produced smooth surfaces with less defects and few nucleation sites at high temperature, and synthesized millimeter sized monolayer $MoSe_2$ single crystals with mobility of up to *ca.* 100 $cm^2 \cdot V^{-1} \cdot s^{-1}$ [Fig.5(A)—(C)]. Another effective approach to reduce the density of nucleation is based on the etching of partially unstable $MoS_2$ nucleation points with $O_2$ during $MoS_2$ growth. With this approach, monolayered $MoS_2$ single crystals with the single domain size of *ca.* 350 μm and a mobility up to 90 $cm^2 \cdot V^{-1} \cdot s^{-1}$ were obtained on sapphire substrate [Fig.5(D)—(F)][60]. Single-crystalline $MoS_2$ monolayer over 300 μm was also synthesized by suppressing the nuclei density by modulating the distance between growth substrate and precursors[61]. In addition, the formation process of $MoS_2$ flakes was observed by *in situ* transmission electron microscope (TEM)[62], which is important for understanding the detailed growth mechanism.

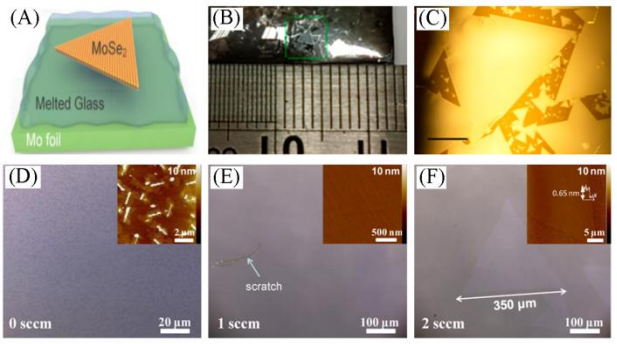


**Fig.5 Schematics(A), photograph(B) and optical images(C) of $MoSe_2$ crystals grown on molten glass(scale bar in 500 μm)[59], optical and AFM images of $MoS_2$ grown on sapphire substrates with 0 sccm(D), 1 sccm(E), and 2 sccm(F) $O_2$, respectively[60]**

(A) Copyright 2017, Journal of the American Chemical Society; (B) Copyright 2015, Journal of the American Chemical Society.

### *3.2.2 Accelerate the Growth Rates*

In the growth process of 2D TMDCs on surface, the precursor molecules or the intermediate products in the gas phase are adsorbed by nucleation sites on the substrates, and then grow up into single crystals through epitaxial growth. So the growth rate significantly affects the size of the obtained 2D single crystals and it is feasible to increase the size of the 2D TMDCs single crystals by simply accelerating the growth rate. Liu *et al.*[63] employed fluorine to promote the growth dynamics during the synthesis of graphene and $WS_2$ by CVD, and the growth rate of graphene can be increased to *ca.* 200 μm/s[Fig.6(A)—(C)]. Particularly, the size of the domains of $WS_2$ single crystals increased from *ca.* 1 μm without fluoride to *ca.* 100 μm with fluoride, and the growth rate increased from 0.2 μm/min to 20 μm/min[Fig.6(D) and (H)]. Zhang *et al.*[64]

utilized molybdenum foil as the precursor and sodium-calcium glass as the growth substrate, and obtained monolayered $MoS_2$ polycrystalline film[Fig.6(E)—(G)] and large single domains of over 400 μm, with a growth rate of *ca.* 50 μm/min. They attributed the rapid growth of $MoS_2$ to the introduction of sodium from the growth substrates. These promoters were involved in the gas-phase reactions and lowered the growth energy barriers and therefore, dramatically increased the growth rates and enlarged the size of the obtained single crystals.

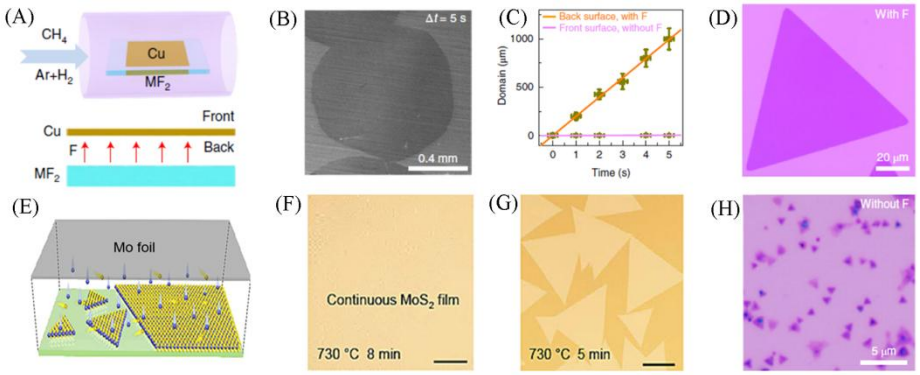


**Fig.6 Schematics for the CVD growth of graphene with fluoride(A) and the optical image of the obtained graphene(B), effect of fluoride on the fast growth of graphene(C)[63], optical images of $WS_2$ grown with(D) and without(H) fluoride[63], schematic diagram of $MoS_2$ grown on sodium-calcium glass(E) and optical images of $MoS_2$ grown after different growth durations(F, G)[64]**

(A—D, H) Copyright 2019, Nature Chemistry; (E—G) Copyright 2018, Nature Communications.

### 3.2.3 *Orientation Alignment by Surface Engineering*

In addition to the growth of a single crystal over a large area on the growth substrates, an alternative way to the growth of large 2D single crystals is based on merging different single crystalline domains with the same orientation to eliminate the formation of grain boundaries in the final products. The orientations of 2D TMDCs can be tuned by the symmetry of the substrate surface. Kis *et al.*[65] synthesized $MoS_2$ triangular monolayers with orientations of 0° and 60° on sapphire substrate as the results of the lattice matching of sapphire with $MoS_2$[Fig.7(A)]. Gao *et al.*[66] synthesized a homogeneous large-area monolayer $WS_2$ film on gold substrate, and the single domain size of the as-grown $WS_2$ was close to millimeter scale[Fig.7(B) and (C)]. They attributed the successful growth of large $WS_2$ to the gold substrate inhibiting the growth of multi-layer $WS_2$ and reducing the reaction energy barrier. Using liquid metal can break the symmetry of the substrate surface, as the symmetry of the substrate surface mainly comes from periodic lattice arrangement. For example, Lee *et al.*[67] first synthesized a large single crystals of *h*-BN on the liquid gold substrate[Fig.7(D)], and then synthesized $WS_2$ and $MoS_2$ single crystals using the obtained *h*-BN as the substrate. On this

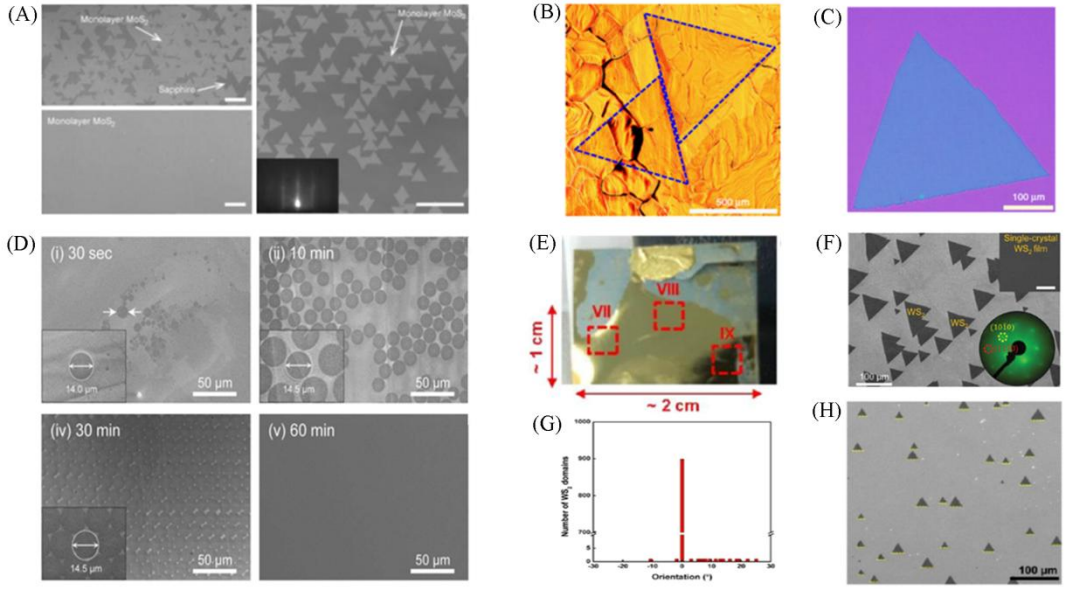


**Fig.7 SEM images of $MoS_2$ grown on sapphire substrates(A)[65], optical images of millimeter scale $WS_2$ grown on gold substrate(B) and transferred to silicon substrate(C)[66], SEM images of *h*-BN grown on liquid gold substrate(D)[67] and optical images(E) and SEM images(F) of $WS_2$ grown on as-grown *h*-BN substrate, crystal domain orientation distributions of $WS_2$ grown on *h*-BN(G)[67] and optical image of $MoS_2$ grown on *h*-BN substrate(H)[67]**

(A) Copyright 2015, ACS Nano; (B, C) Copyright 2015, Nature Communications; (D—H) Copyright 2018, Science.

*h*-BN substrate, the obtained triangular $WS_2$ flakes exhibited almost the same orientation[Fig.7(F) and (G)], and by prolonging the growth time, the individual $WS_2$ merged together and formed large single crystal $WS_2$ film[Fig.7(E)]. They also realized the synthesis of large-area single crystal $MoS_2$ monolayer on *h*-BN grown on liquid gold substrate[Fig.7(H)].

## 4 Conclusions

In summary, although some encouraging progresses have been made on the growth of large 2D single crystals of semiconducting TMDCs, related studies are still at an early stage. The size of CVD grown single crystalline graphene has reached up to meters' scale with very fast growth rates. However, the size of single crystals domains of $MoS_2$ is still within one millimeter. It is urgent to explore the detailed growth mechanism of these 2D TMDCs by combining experimental studies with theoretical calculations to guide the rational design of new growth methods. In addition, more efforts should be made on designing new growth set-up, searching for possible catalysts and promoters, testing appropriate growth substrate, synthesizing new precursors, and carefully optimizing the CVD growth parameters. Meanwhile, subsequent studies with these 2D single crystals should be conducted, such as the nondestructive transfer, patterning and device design, and integration strategies with these high quality ultrathin semiconductors to accelerate their practical applications in high performance devices.

## References


[1] Cooke Y. E., *Engineering Science & Education Journal*, **1998**, *7*, 100

[2] Lundstrom M., *Science*, **2003**, *299*, 210

[3] Ghetti A., *Microelectron Eng.*, **2001**, *59*, 127

[4] Yang P. L., Hook T. B., Oldiges P. J., Doris B. B., *IEEE Trans. Electron Devices*, **2016**, *63*, 3327

[5] Auth C., Allen C., Blattner A., Bergstrom D., Brazier M., Bost M., Buehler M., Chikarmane V., Ghani T., Glassman T., *2012 Symposium on VLSI Technology(VLSIT)*, **2012**, 131

[6] Mak K. F., Shan J., *Nat. Photonics*, **2016**, *10*, 216

[7] Voiry D., Mohite A., Chhowalla M., *Chem. Soc. Rev.*, **2015**, *44*, 2702

[8] Wilson J. A., Yoffe A., *Adv. Phys.*, **1969**, *18*, 193

[9] Yoffe A. D., *Adv. Phys.*, **1993**, *42*, 173

[10] Ling X., Lin Y., Ma Q., Wang Z., Song Y., Yu L., Huang S., Fang W., Zhang X., Hsu A. L., Bie Y., Lee Y. H., Zhu Y., Wu L., Li J., Jarillo-Herrero P., Dresselhaus M., Palacios T., Kong J., *Adv. Mater.*, **2016**, *28*, 2322

[11] Theis T. N., Wong H. S. P., *Comput. Sci. Eng.*, **2017**, *19*, 41

[12] Pop E., *Nano Res.*, **2010**, *3*, 147

[13] Saha P., Banerjee P., Dash D. K., Sarkar S. K., *J. Mater. Eng. Perform.*, **2018**, *27*, 2708

[14] Wolf S., *Sunset Beach, CA*, **1990**, *11290*, 321

[15] Wang J., Zheng H., Xu G., Sun L., Hu D., Lu Z., Liu L., Zheng J., Tao C., Jiao L., *J. Am. Chem. Soc.*, **2016**, *138*, 16216

[16] Li L. J., Lu W. J., Liu Y., Qu Z., Ling L. S., Sun Y. P., *Physica C*, **2013**, *492*, 64

[17] Valla T., Fedorov A., Johnson P., Glans P., Mcguinness C., Smith K., Andrei E., Berger H., *Phys. Rev. Lett.*, **2004**, *92*, 086401

[18] Tissen V., Osorio M., Brison J. P., Nemes N., García-Hernández M., Cario L., Rodiere P., Vieira S., Suderow H., *Phys. Rev. B*, **2013**, *87*, 134502

[19] Voiry D., Goswami A., Kappera R., Silva C., Kaplan D., Fujita T., Chen M., Asefa T., Chhowalla M., *Nat. Chem.*, **2015**, *7*, 45

[20] Zheng J., Yan X., Lu Z., Qiu H., Xu G., Zhou X., Wang P., Pan X., Liu K., Jiao L., *Adv. Mater.*, **2017**, *29*, 1604540

[21] Liu L., Wu J., Wu L., Ye M., Liu X., Wang Q., Hou S., Lu P., Sun L., Zheng J., Xing L., Gu L., Jiang X., Xie L., Jiao L., *Nat. Mater.*, **2018**, *17*, 1108

[22] Ye G., Gong Y., Lin J., Li B., He Y., Pantelides S. T., Zhou W., Vajtai R., Ajayan P. M., *Nano Lett.*, **2016**, *16*, 1097

[23] Wang Q. H., Kalantar-Zadeh K., Kis A., Coleman J. N., Strano M. S., *Nat. Nanotechnol*, **2012**, *7*, 699

[24] Geim A. K., Grigorieva I. V., *Nature*, **2013**, *499*, 419

[25] Miro P., Audiffred M., Heine T., *Chem. Soc. Rev.*, **2014**, *43*, 6537

[26] Manzeli S., Ovchinnikov D., Pasquier D., Yazyev O. V., Kis A., *Nat. Rev. Mater.*, **2017**, *2*, 17033

[27] Hu D., Zhao T., Ping X., Zheng H., Xing L., Liu X., Zheng J., Sun L., Gu L., Tao C., Wang D., Jiao L., *Angew. Chem. Int. Ed. Engl.*, **2019**, *58*, 6977

[28] Jariwala D., Sangwan V. K., Late D. J., Johns J. E., Dravid V. P., Marks T. J., Lauhon L. J., Hersam M. C., *Appl. Phys. Lett.*, **2013**, *102*, 173107

[29] Huang J. K., Pu J., Hsu C. L., Chiu M. H., Juang Z. Y., Chang Y. H., Chang W. H., Iwasa Y., Takenobu T., Li L. J., *ACS Nano*, **2014**, *8*, 923

[30] Wang X., Gong Y., Shi G., Chow W. L., Keyshar K., Ye G., Vajtai R., Lou J., Liu Z., Ringe E., Tay B. K., Ajayan P. M., *ACS Nano*, **2014**, *8*, 5125

[31] Ovchinnikov D., Allain A., Huang Y. S., Dumcenco D., Kis A., *ACS Nano*, **2014**, *8*, 8174

[32] Radisavljevic B., Radenovic A., Brivio J., Giacometti V., Kis A., *Nat. Nanotechnol*, **2011**, *6*, 147

[33] Liu X., Hu J., Yue C., Della Fera N., Ling Y., Mao Z., Wei J., *ACS Nano*, **2014**, *8*, 10396

[34] Zhao Y., Qiao J., Yu Z., Yu P., Xu K., Lau S. P., Zhou W., Liu Z., Wang X., Ji W., Chai Y., *Adv. Mater.*, **2017**, *29*, 1604230

[35] Zhou C., Zhao Y., Raju S., Wang Y., Lin Z., Chan M., Chai Y., *Adv. Funct. Mater.*, **2016**, *26*, 4223

[36] Kappera R., Voiry D., Yalcin S. E., Branch B., Gupta G., Mohite A. D., Chhowalla M., *Nat. Mater.*, **2014**, *13*, 1128

[37] Zhang Y., Yao Y. Y., Sendeku M. G., Yin L., Zhan X. Y., Wang F., Wang Z. X., He J., *Adv. Mater.*, **2019**, *31*, 1901694

[38] Liu T., Liu S., Tu K. H., Schmidt H., Chu L., Xiang D., Martin J., Eda G., Ross C. A., Garaj S., *Nat. Nanotechnol*, **2019**, *14*, 223

[39] Cui Y., Xin R., Yu Z., Pan Y., Ong Z. Y., Wei X., Wang J., Nan H., Ni Z., Wu Y., Chen T., Shi Y., Wang B., Zhang G., Zhang Y. W., Wang X., *Adv. Mater.*, **2015**, *27*, 5230

[40] Das S., Chen H. Y., Penumatcha A. V., Appenzeller J., *Nano Lett.*, **2013**, *13*, 100

[41] Cho S., Kim S., Kim J. H., Zhao J., Seok J., Keum D. H., Baik J., Choe D. H., Chang K. J., Suenaga K., Kim S. W., Lee Y. H., Yang H., *Science*, **2015**, *349*, 625

[42] Desai S. B., Madhvapathy S. R., Sachid A. B., Llinas J. P., Wang Q., Ahn G. H., Pitner G., Kim M. J., Bokor J., Hu C., Wong H. P., Javey A., *Science*, **2016**, *354*, 99

[43] Zhang H., *ACS Nano*, **2015**, *9*, 9451

[44] Liu H., Neal A. T., Ye P. D., *ACS Nano*, **2012**, *6*, 8563

[45] Kang K., Xie S., Huang L., Han Y., Huang P. Y., Mak K. F., Kim C.

J., Muller D., Park J., *Nature*, **2015**, *520*, 656

[46] Lin Z., Liu Y., Halim U., Ding M., Liu Y., Wang Y., Jia C., Chen P., Duan X., Wang C., Song F., Li M., Wan C., Huang Y., Duan X., *Nature*, **2018**, *562*, 254

[47] Mennel L., Symonowicz J., Wachter S., Polyushkin D. K., Molina-Mendoza A. J., Mueller T., *Nature*, **2020**, *579*, 62

[48] Yazyev O. V., Louie S. G., *Nat. Mater.*, **2010**, *9*, 806

[49] Peng J., Wu J., Li X., Zhou Y., Yu Z., Guo Y., Wu J., Lin Y., Li Z., Wu X., Wu C., Xie Y., *J. Am. Chem. Soc.*, **2017**, *139*, 9019

[50] Kulkarni S. S., Wang C. C., Sabbavarapu N. M., Podilapu A. R., Liao P. H., Hung S. C., *Chem. Rev.*, **2018**, *118*, 8025

[51] Zhou H., Wang C., Shaw J. C., Cheng R., Chen Y., Huang X., Liu Y., Weiss N. O., Lin Z., Huang Y., Duan X., *Nano Lett.*, **2015**, *15*, 709

[52] Hu D., Xu G., Xing L., Yan X., Wang J., Zheng J., Lu Z., Wang P., Pan X., Jiao L., *Angew. Chem. Int. Ed. Engl.*, **2017**, *56*, 3611

[53] Li G., Zhang Y. Y., Guo H., Huang L., Lu H., Lin X., Wang Y. L., Du S., Gao H. J., *Chem. Soc. Rev.*, **2018**, *47*, 6073

[54] Li X., Cai W., An J., Kim S., Nah J., Yang D., Piner R., Velamakanni A., Jung I., Tutuc E., Banerjee S. K., Colombo L., Ruoff R. S., *Science*, **2009**, *324*, 1312

[55] Liu K. K., Zhang W., Lee Y. H., Lin Y. C., Chang M. T., Su C. Y., Chang C. S., Li H., Shi Y., Zhang H., Lai C. S., Li L. J., *Nano Lett.*, **2012**, *12*, 1538

[56] Wang S. S., Rong Y. M., Fan Y., Pacios M., Bhaskaran H., He K., Warner J. H., *Chem. Mater.*, **2014**, *26*, 6371

[57] van der Zande A. M., Huang P. Y., Chenet D. A., Berkelbach T. C., You Y., Lee G. H., Heinz T. F., Reichman D. R., Muller D. A., Hone J. C., *Nat. Mater.*, **2013**, *12*, 554

[58] Hao Y., Bharathi M. S., Wang L., Liu Y., Chen H., Nie S., Wang X., Chou H., Tan C., Fallahazad B., Ramanarayan H., Magnuson C. W., Tutuc E., Yakobson B. I., McCarty K. F., Zhang Y. W., Kim P., Hone J., Colombo L., Ruoff R. S., *Science*, **2013**, *342*, 720

[59] Chen J., Zhao X., Tan S. J., Xu H., Wu B., Liu B., Fu D., Fu W., Geng D., Liu Y., Liu W., Tang W., Li L., Zhou W., Sum T. C., Loh K. P., *J. Am. Chem. Soc.*, **2017**, *139*, 1073

[60] Chen W., Zhao J., Zhang J., Gu L., Yang Z., Li X., Yu H., Zhu X., Yang R., Shi D., Lin X., Guo J., Bai X., Zhang G., *J. Am. Chem. Soc.*, **2015**, *137*, 15632

[61] Lin Z., Zhao Y., Zhou C., Zhong R., Wang X., Tsang Y. H., Chai Y., *Sci. Rep.*, **2015**, *5*, 18596

[62] Fei L., Lei S., Zhang W. B., Lu W., Lin Z., Lam C. H., Chai Y., Wang Y., *Nat. Commun.*, **2016**, *7*, 12206

[63] Liu C., Xu X., Qiu L., Wu M., Qiao R., Wang L., Wang J., Niu J., Liang J., Zhou X., Zhang Z., Peng M., Gao P., Wang W., Bai X., Ma D., Jiang Y., Wu X., Yu D., Wang E., Xiong J., Ding F., Liu K., *Nat. Chem.*, **2019**, *11*, 730

[64] Yang P., Zou X., Zhang Z., Hong M., Shi J., Chen S., Shu J., Zhao L., Jiang S., Zhou X., Huan Y., Xie C., Gao P., Chen Q., Zhang Q., Liu Z., Zhang Y., *Nat. Commun.*, **2018**, *9*, 979

[65] Dumcenco D., Ovchinnikov D., Marinov K., Lazic P., Gibertini M., Marzari N., Lopez Sanchez O., Kung Y. C., Krasnozhon D., Chen M. W., Bertolazzi S., Gillet P., Fontcuberta I Morral A., Radenovic A., Kis A., *ACS Nano*, **2015**, *9*, 4611

[66] Gao Y., Liu Z., Sun D. M., Huang L., Ma L. P., Yin L. C., Ma T., Zhang Z., Ma X. L., Peng L. M., Cheng H. M., Ren W., *Nat. Commun.*, **2015**, *6*, 8569

[67] Lee J. S., Choi S. H., Yun S. J., Kim Y. I., Boandoh S., Park J. H., Shin B. G., Ko H., Lee S. H., Kim Y. M., Lee Y. H., Kim K. K., Kim S. M., *Science*, **2018**, *362*, 817